

RESEARCH ARTICLE

Interruption of an *MSH4* homolog blocks meiosis in metaphase I and eliminates spore formation in *Pleurotus ostreatus*

Brian Lavrijssen¹, Johan P. Baars¹, Luis G. Lugones², Karin Scholtmeijer^{1*}, Narges Sedaghat Telgerd¹, Anton S. M. Sonnenberg¹, Arend F. van Peer¹

¹ Plant Breeding Department, Wageningen University and Research, Wageningen, The Netherlands,

² Microbiology Faculty of Science, Utrecht University, Utrecht, The Netherlands

* karin.scholtmeijer@wur.nl



Abstract

Pleurotus ostreatus, one of the most widely cultivated edible mushrooms, produces high numbers of spores causing severe respiratory health problems for people, clogging of filters and spoilage of produce. A non-sporulating commercial variety (SPOPPO) has been successfully introduced into the market in 2006. This variety was generated by introgression breeding of a natural mutation into a commercial variety. Our cytological studies revealed that meiosis in the natural and derived sporeless strains was blocked in metaphase I, apparently resulting in a loss of spore formation. The gene(s) underlying this phenotype were mapped to an 80 kb region strongly linked to sporelessness and identified by transformation of wild type genes of this region into a sporeless strain. Sporulation was restored by re-introduction of the DNA sequence encoding the *P. ostreatus* meiotic recombination gene *MSH4* homolog (*poMSH4*). Subsequent molecular analysis showed that *poMSH4* in the sporeless *P. ostreatus* was interrupted by a DNA fragment containing a region encoding a CxC5/CxC6 cysteine cluster associated with Copia-type retrotransposons. The block of meiosis in metaphase I by a *poMSH4* null mutant suggests that this protein plays an essential role in both Class I and II crossovers in mushrooms, similar to animals (mice), but unlike in plants. *MSH4* was previously shown to be a target for breeding of sporeless varieties in *P. pulmonarius*, and the null mutant of the *MSH4* homolog of *S. commune* (*scMSH4*) confers an extremely low level of spore formation. We propose that *MSH4* homologs are likely to be a breeding target for sporeless strains both within *Pleurotus* sp. and in other *Agaricales*.

OPEN ACCESS

Citation: Lavrijssen B, Baars JP, Lugones LG, Scholtmeijer K, Sedaghat Telgerd N, Sonnenberg ASM, et al. (2020) Interruption of an *MSH4* homolog blocks meiosis in metaphase I and eliminates spore formation in *Pleurotus ostreatus*. PLoS ONE 15(11): e0241749. <https://doi.org/10.1371/journal.pone.0241749>

Editor: Arthur J. Lustig, Tulane University Health Sciences Center, UNITED STATES

Received: July 9, 2020

Accepted: October 21, 2020

Published: November 4, 2020

Peer Review History: PLOS recognizes the benefits of transparency in the peer review process; therefore, we enable the publication of all of the content of peer review and author responses alongside final, published articles. The editorial history of this article is available here: <https://doi.org/10.1371/journal.pone.0241749>

Copyright: © 2020 Lavrijssen et al. This is an open access article distributed under the terms of the [Creative Commons Attribution License](https://creativecommons.org/licenses/by/4.0/), which permits unrestricted use, distribution, and reproduction in any medium, provided the original author and source are credited.

Data Availability Statement: All relevant data are within the manuscript and its [Supporting Information](#) files.

Introduction

During the cultivation of mushrooms, fruiting bodies can release a large number of spores. These spores can cause severe problems for people harvesting and handling the crop. Repeated exposure to high spore numbers causes extrinsic allergic alveolitis, an inflammation of the alveoli in the lung provoked by inhalation of spores [1]. In addition, spores clog filters in the climate-control system and play an important role in spreading viral diseases [2, 3]. *Pleurotus ostreatus* (Oyster mushroom), one of the most widely cultivated edible mushrooms [4], is

Funding: The authors received no specific funding for this work.

Competing interests: The authors have declared that no competing interests exist.

especially known for its heavy sporulation, and spore densities of 10^{10} spores/m³ are easily achieved [5]. Because of this high number of spores and the inevitable consequences, there is a strong demand for non-sporulating commercial strains.

Spontaneous sporeless mutants of basidiomycetes have been found from natural populations in *Coprinopsis cinerea* [6], *Schizophyllum commune* [7], *Lentinula edodes* [8], *Agrocybe salicicola* [9], *Pleurotus ostreatus* [10] and *Pleurotus pulmonarius* [11]. Sporeless mushroom strains have also been generated successfully by mutagenesis using chemical treatment and UV irradiation in *C. cinerea* [12], *Agrocybe cylindracea* [13], *P. pulmonarius*, *P. ostreatus* [14, 15], *Pleurotus eryngii* [16], *Pleurotus florida* and *Pleurotus sajor-caju* [17]. These sporeless mutants are important as breeding material in developing sporeless strains for commercial cultivation. It appeared, however, difficult to restore yield and quality in these mutants to an acceptable level by breeding and there have been, to our knowledge, only three sporeless strains commercially produced: *P. ostreatus* SPOppo [18, 19], *P. eryngii* [20] and *A. cylindracea* [13]. For the *P. ostreatus* SPOppo variety, a breeding program based on a spontaneous sporeless *P. ostreatus* mutant, ATCC58937 (F42 x 11; [10]) and commercial variety HK35 was performed. In this breeding program, Baars *et. al.* [21] studied the inheritance of the sporeless phenotype (100% reduction of spores) and concluded that it is recessive, and mapped in both constitutive haploid genomes of the sporeless mutant, on the same chromosome and at the same locus. The sporeless phenotype further mapped on the same chromosome as the *A* mating-type. The breeding program yielded a commercially acceptable sporeless strain although it has a somewhat deviating morphology, in particular, the fruiting bodies show a disturbed orientation. The intention of the present research was to identify and characterize the gene(s) responsible for the sporeless phenotype in *P. ostreatus*. This will facilitate breeding for additional sporeless varieties, allowing a more accurate selection and reduction of linkage drag. If the identified gene(s) similarly participate in sporulation in other (edible) mushroom forming fungi, these could also be used to develop sporeless varieties in other species.

The offspring (spores) in mushrooms are the outcome of meiosis and it has been shown previously that blockage of this process can also eliminate or reduce the production of spores. Deletion of the meiotic genes *DMC1* and *SPO11* impaired sporulation in *P. ostreatus* and *C. cinerea* respectively [22, 23]. In yeast, the *RAD51* gene is involved in meiosis and its *P. ostreatus* homolog showed elevated expression levels in lamellae/basidia, although expression levels are similar when compared between a sporulating strain and the sporeless mutant [24]. Another meiotic gene, *MER3*, is required for synaptonemal complex formation and a null mutant reduces spore formation dramatically in *C. cinerea* [25]. Okuda *et. al.* [26] describe a defective *STPP1* gene, a *P. pulmonarius MSH4* homolog, to be responsible for the absence of spores in a sporeless mutant. Here we show that the absence of spores in the commercial *P. ostreatus* variety SPOppo is caused by a defect *MSH4* homolog (defined as *poMSH4* for simplicity), that has been disrupted by an insertion of a transposon-like fragment. A cytological study showed that meiosis in the *P. ostreatus* strain SPOppo is blocked at metaphase I. We also show that an artificial disruption of the *MSH4* homolog of *S. commune* (defined as *scMSH4*), a non-*Pleurotus* sp., diminished sporulation to less than 0.1% of the wild type.

Materials and methods

Strains and mapping population

Two *Pleurotus ostreatus* strains were used: a normal sporulating dikaryotic (Sp⁺ dikaryon) strain N001 [27] with its two constituent monokaryons PC9 (Sp⁺hap1) and PC15 (Sp⁺hap2) and a non-sporulating dikaryotic mutant ATCC58937 (F42 x 11; [10]) with its two constituent monokaryons EP25 (Sp⁻hap1) and EP57 (Sp⁻hap2). Both monokaryons (Sp⁻hap1 and Sp⁻hap2)

are carriers of the sporeless trait, resulting in a homozygous locus for this recessive trait. A mapping population was generated by isolating 188 monokaryotic progeny (BKK population) of a cross between Sp⁺hap2 and Sp⁻hap2. Sp⁺hap2 was selected as a parent for the mapping population since its whole genome was sequenced (http://genome.jgi.doe.gov/PleosPC15_2; [28]). This population was used to determine segregation of Single Nucleotide Polymorphism (SNP) markers and Cleaved Amplified Polymorphic Sequences (CAPS) markers and to map the phenotypes sporelessness, disturbed orientation of fruiting bodies and *A* and *B* mating-type. All strains used, were maintained in vials containing perlite in 1% malt extract and 2.5% glycerol and stored in liquid nitrogen. For short term storage, strains were maintained on malt extract agar (MEA; 1% malt extract and 2% agar) in slants at 4°C. Vegetative mycelium was grown on MEA at 24°C.

The sequenced monokaryotic *Schizophyllum commune* strain H4-8 (FGSC #9219) and its isogenic derivatives H4-8b, c and d were used as wild-type strains. For generating knock-outs, the dikaryotic $\Delta ku80$ strain was used (H4-8/H4-8b background; [29]). In this strain the *ku80* gene is deleted by integration of a hygromycin resistance cassette, resulting in abolishment of ectopic integration upon transformation. Strains were grown at 25°C on minimal medium [30]. When needed minimal medium was supplemented with nourseothricin (8 µg/ml), phleomycin (5 µg/ml) or hygromycin (5 µg/ml).

Phenotyping

The sporeless phenotype was assessed after crossing each individual of the mapping population with the monokaryon Sp⁻hap1. Spawn of all crosses was prepared by inoculating sterile sorghum seeds (70 g/box) with a 2 x 2 cm agar piece from a fully grown petri dish and incubation at 24°C for 10–11 days. Bags (Polypropylene 3T bags with BN filter; Unicorn Bags) containing 1 kg of wheat straw substrate were inoculated using 35–40 grams of spawn, sealed and incubated at 24°C for 20 to 30 days in the dark. When fully colonized, fruiting was induced by changing the environmental conditions to 15°C, 90% relative humidity, max. 600 ppm CO₂ and 12/24 hours of light, while a slit was made on each side of the package. Fruiting bodies were evaluated for their orientation and the gills were microscopically examined for presence of spores on the basidia.

Sequencing, SNP selection and genotyping

High molecular genomic DNA of Sp⁻hap2 was extracted using the DNeasy Plant Kit (Qiagen, Germany) according to the suppliers protocol and sequenced using Illumina Genome Analyzer II Paired-End Sequencing (ServiceXS, The Netherlands). For genotyping, the sequencing reads were mapped against the reference genome assembly of Sp⁺hap2 and Single Nucleotide Polymorphisms (SNP's) were identified using NextGene software (SoftGenetics State College, PA, USA). SNP's were selected, evenly distributed over the whole genome with 100 kb intervals. For scaffold 3, harboring the sporeless locus, SNP's were selected with about 50 kb intervals.

Genomic DNA was extracted from the individuals of the BKK mapping population using the Wizard[®] Magnetic 96 DNA Plant System (Promega, USA) and genotyped using the Illumina GoldenGate Assay (ServiceXS, The Netherlands). JoinMap 4 software [31] was used for linkage mapping.

For *de novo* assembly of the whole genome sequence of Sp⁻hap2, high molecular genomic DNA was extracted as described by van Peer *et al.* [32] but using 10–20 mg of lyophilized mycelium per sample. DNA was dissolved in 110 µl TE containing 1 mg/ml RNase A and after 1–2 hours of incubation at 37°C, the entire extraction protocol was repeated. The

extracted DNA was subsequently purified using the Genomic DNA Clean & Concentrator Kit (Zymo Research, USA) according to the suppliers protocol. Prior to library construction according to the “Procedure & Checklist—Preparing >30 kb Libraries Using SMRTbell[®] Express Template Preparation Kit” (Pacific Biosciences, USA), DNA was sheared using the Megaruptor. The library was sequenced on the PacBio Sequel using the Sequel 6.0 chemistry and data were collected with SMRT Link v.6.0.0 (Pacific Biosciences, USA). The subreads were assembled using Canu version 1.7 software [33] resulting in 62 contigs with a total assembly size of 35.0 Mbp.

Construction of a *poMSH4* expression vector and transformation of *P. ostreatus*

Primers were designed based on the Sp⁺hap2 sequence to amplify genomic regions containing at least one identified gene, including a 1 kb region upstream as a promoter region and 500 bp downstream as a terminator region (S1 Table). Target regions were amplified from the Sp⁺hap2 genome using Phusion DNA Polymerase (Finnzymes, Finland) according to the suppliers protocol, purified and ligated with the pGEM[®]-T Easy Vector System (Promega, USA). The correctness of the sequence of the constructs was confirmed by sequencing.

For protoplast generation, mycelium of the non-sporulating dikaryotic mutant ATCC58937 (Sp⁻dikaryon) was grown in liquid culture [34] and digested according to the method as described by Binnering *et al.* [35] but using a lysing enzyme solution containing 50 mM maleate buffer (pH 5.5), 0.5 M mannitol and 1 mg/ml *Trichoderma harzianum* cell wall lytic enzymes [36]. Transformation of the protoplasts was carried out as described by [37]. The candidate gene constructs were co-transformed with the carboxin selection marker construct pTM1 [38]; 1 µg pTM1 was used in combination with 5 µg candidate gene construct. After regeneration for 7 days, 24 carboxin resistant colonies were transferred to fresh MEA containing carboxin (2 mg/l) and microscopically screened for the presence of clamp connections. Heterokaryotic transformants were screened for the presence of the constructs via PCR using construct specific primers (S2 Table).

For fructification of the transformants, spawn was prepared as described before. For each transformant, about 300 g of wheat straw substrate was mixed with 15–20 g of spawn and transferred to a box (ECO2box white filter, Duchefa Biochemie b.v.). Enough substrate was added to fill the box tightly. Inoculated substrate was incubated at 24°C for 11–22 days. When fully colonized, boxes were transferred to a climate room (15°C, 90% relative humidity, max. 600 ppm CO₂, 12/24 hours of light) and the air filter in the lid was cut to induce fruiting. Gills were microscopically examined at 20x magnification for presence of spores using a Zeiss Axio Scope.A1 microscope with Zeiss AxioCam ERc 5s digital camera. Gill tissue and fruiting bodies were collected and immediately transferred to liquid nitrogen. For each transformant with restored sporulation, a tissue culture and spore print were made.

Construction of a *scMSH4* knock-out in *S. commune*

A protein sequence homolog of *poMSH4* was searched in the *S. commune* H4-8 sequence database (<http://genome.jgi-psf.org/Schco3/Schco3.home.html>). Protein ID 1186310 (<http://genome.jgi-psf.org/cgi-bin/dispGeneModel?db=Schco3&id=1186310>) was found to have 63% identity with *poMSH4* (E value = 0.0). In order to delete the gene encoding this protein, a pDelcas derivative (pDelMSH4) was made following the protocol described by Ohm *et al.* [39], containing the *S. commune* phleomycin and nourseothricin resistance cassette. The flanking sequences of *scMSH4* were amplified using the primers Δmsh4ufw and Δmsh4urv for the upstream flank and Δmsh4dfw and Δmsh4drv for the downstream flank (S3 Table) and cloned

on either side of the nourseothricin resistance cassette. The $\Delta ku80$ strain was transformed as described by de Jong *et al.* [29] with the modification that, instead of using monokaryotic mycelium to obtain the protoplasts, germinated monokaryotic spores from the $\Delta ku80$ dikaryon were used. Potential candidates, which grew on nourseothricin but not on phleomycin, were analyzed by PCR using primers *msh4ufscf* and *pdkufscf* to test insertion in the upstream region and *pdkdfscf* and *msh4dfscf* for insertion in the downstream flank (S3 Table).

For fructification, sorghum grains were inoculated with mycelium and incubated at 30°C in the dark until fully colonized. Colonized grains were transferred to small burlap bags, hung in a beaker above a small amount of water, sealed with parafilm and placed at room temperature in the light. After fructification, fruiting bodies were cut from the bag, transferred to 50 ml Greiner tubes and weighted. To each tube 2 ml of 0.1% Tween80 was added and tubes were placed under vacuum for 40 min. After shaking for 15 min., the spore suspension was transferred to Eppendorf tubes and centrifuged for 5 min. at 13,300 rpm. Spores were resuspended in 100 μ l and 50 μ l of 0.5x T₁₀E_{0.1} for the wild type and $\Delta\Delta MSH4$ respectively. Spores were counted using a Bürker counting chamber.

RNA extraction, cloning and sequencing

For total RNA extraction, gill tissue was separated from cap tissue of fruiting bodies of *P. ostreatus* N001 (Sp⁺ dikaryon) and ATCC58937 (Sp⁻ dikaryon), immediately frozen using liquid nitrogen and stored at -80°C until use. RNA was extracted according to the method described by Sokolovsky *et al.* [40]. Full length cDNA was generated from total RNA with the SuperScript[®] III First-Strand Synthesis System for RT-PCR (Invitrogen) according to the manufacturers protocol using Oligo(dT)₂₀ primers and random hexamers. The full length *poMSH4* was amplified with primer pair *MSH4_For* (5' -ATGCAAGCCTCTCGTCCAACAAC-3') and *MSH4_Rev* (5' -TTACATTACAAAGAGCTTTGCTA-3'), cloned with the pGEM[®]-T Easy Vector System (Promega, USA) and sequenced by GATC Biotech.

Cytological analysis

For light microscopy, the Giemsa staining method was used as described by Obatake *et al.* [16] using 4CF-1G Double aldehyde (Formaldehyde 35% 100 ml/l; Glutardialdehyde 25% 40 ml/l; NaOH 2.7 g/l; NaH₂PO₄.H₂O 11.6 g/l) as a fixative. Following staining, the tissue was dehydrated by passing through a series of graded ethanol baths and embedded into Methacrylate using Technovit[®] 7100 GMA embedding. Sections of 6–8 μ m thickness were mounted on glass slides and again stained with 1:25 Giemsa-phosphate buffer solution (pH 7) for at least 2 hours. After staining, the samples were washed with tap water and dried. A coverslip was mounted after applying Euparal to the sample. The tissue was examined using a Zeiss Axio-Phot light microscope with a Leica DFC340 FX digital camera.

Results

Identification of candidate genes involved in sporulation of *P. ostreatus*

We previously showed that the sporeless phenotype was recessive and mapped to the same genomic region in both nuclei of the mutant strain ATCC58937; monokaryons Sp⁺hap1 and Sp⁻hap2 [21]. In order to fine-map the region linked to the sporeless phenotype, SNP markers were generated. For this, the sequencing reads of Sp⁻hap2 were mapped against the whole genome sequence of wild-type monokaryon Sp⁺hap2 as a reference, resulting in a total of 212,832 called variants. For genetic mapping, 384 SNP's were selected of which 98 evenly distributed over scaffold 3, harboring the sporeless locus and the *A* mating-type locus. In

addition, 3 CAPS-markers were selected on this scaffold. A mapping population of 188 monokaryotic offspring of a cross between Sp⁺hap2 and Sp⁻hap2 was used to generate a genetic map, consisting of 12 linkage groups covering 1050 cM, on average 32.7 kb/cM (S1 Fig; Adapted version of the map previously published by Sivolapova *et.al.* [41]). All 188 individuals were crossed with Sp⁻hap1 and cultured in duplicate to be screened for sporulation and orientation of fruiting bodies. The phenotypes *A* mating-type, *B* mating-type, sporelessness and disturbed orientation of fruiting bodies were added to the map. As expected, the sporeless phenotype and the *A* mating-type were part of the same linkage group; linkage group 3 (138.7 cM; Fig 1). The disturbed orientation of fruiting bodies was tightly linked to the sporeless phenotype. Sporelessness mapped between SNP-marker 3_975676 and 3_1066945, a 87 kb region. Additional fine mapping reduced the relevant region to 78.9 kb. Using the Sp⁺hap2 genome annotation (http://genome.jgi.doe.gov/PleosPC15_2; [28]), 27 predicted genes were identified in this region, of which 3 genes were predicted to play a role in transcription, replication, recombination and DNA repair. These were the main candidates for playing a role in spore production (Table 1) based on the observation of a blocked meiosis (see below).

Sporulation of *P. ostreatus* is restored by transformation of wild type *poMSH4*

Eleven constructs were made representing in total 23 of the 27 Sp⁺hap2 genes from the same 78.9 kb region that was mapped to the sporeless phenotype in Sp⁻ strains, each construct containing up to 5 genes. Protoplasts of the ATCC58937 (Sp⁻ dikaryon) were transformed with each construct, and 24 confirmed transformants per construct were screened for the presence of clamp connections (dikaryons). Clamp connections were observed in 70–90% of the confirmed transformants. Fruiting bodies were cultivated for 5 dikaryotic transformants per construct (in duplicate) and gills of fruiting bodies were microscopically examined for (lack of) spores. A single construct restored sporulation, containing a unique gene and a second gene that was also present in another construct. A final construct containing the only remaining candidate gene restored sporulation in all Sp⁻ dikaryon transformants (Fig 2). Notably, with restoration of sporulation also the proper orientation of the fruiting bodies was restored. The gene restoring sporulation in the Sp⁻ host was identified as a homolog of MutS homolog 4 (*MSH4*), a meiosis specific gene required for reciprocal recombination and proper segregation of homologous chromosomes during meiosis I. The genomic DNA sequence of the Sp⁺hap2 *poMSH4* (JGI protein ID 1101251; https://mycocosm.jgi.doe.gov/cgi-bin/dispGeneModel?db=PleosPC15_2&id=1101251) was 3,864 bp in length. Alignment with the 2,556 bp total RNA sequence of the sporulating *P. ostreatus* N001 strain (Sp⁺ dikaryon) revealed that the *poMSH4* gene contained 26 exons ranging in size between 8 and 300 bp and encoded a protein of 851 amino acids (S1 File). A BLAST search of the *poMSH4* encoded sequence to Sp⁺hap2 revealed the presence of only one copy of this gene.

In the sporeless *P. ostreatus* strain *poMSH4* is interrupted by a DNA fragment that can be associated with a Copia-type retrotransposon

The genomic *poMSH4* sequence of Sp⁺hap2 was blasted against the Sp⁻hap2 *de novo* assembly (S2 File), resulting in a match with contig 00000008 (S2 File contig 00000008), on which the Sp⁻hap2 *poMSH4* sequence was found to be interrupted by a 6,792 bp DNA fragment. To study the origin and nature of this integrated DNA fragment (from here on called “insert”), a 75 kb region of contig 00000008 surrounding the interrupted *poMSH4* gene (S3 File) was aligned to the well annotated genome of Sp⁺hap2 (http://genome.jgi.doe.gov/PleosPC15_2; [28]). The corresponding region of the annotated genome of Sp⁺hap2 scaffold 3 (Fig 3A; S1

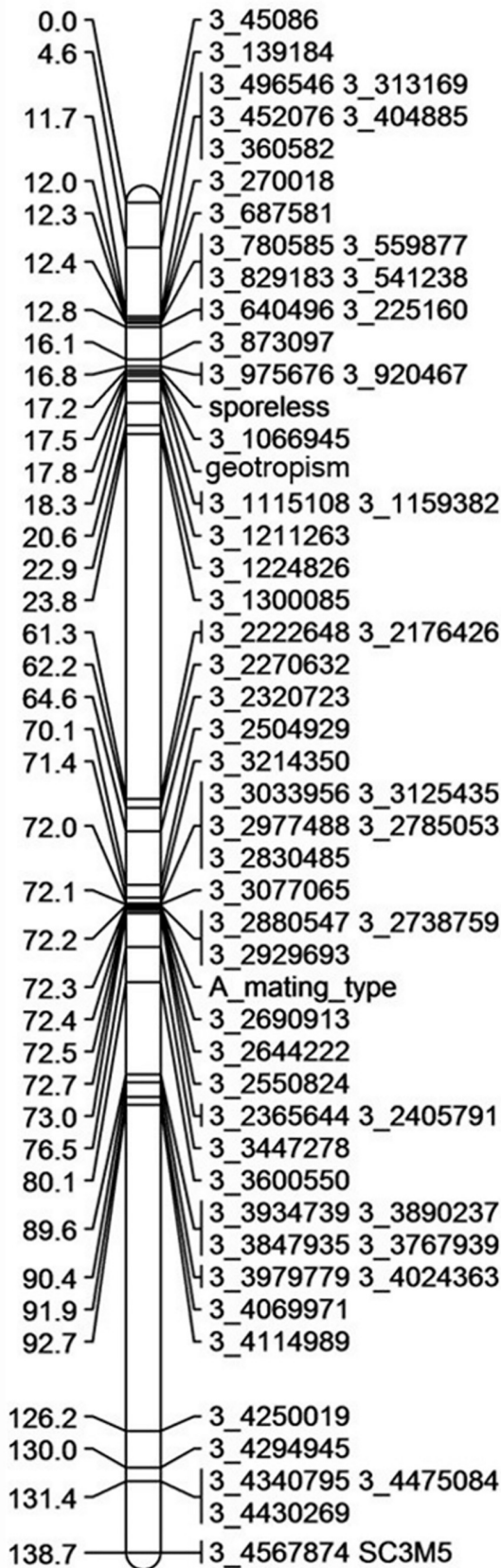


Fig 1. Linkage group 3 of the genetic linkage map of Sp⁺Hap2 x Sp⁻Hap2. This linkage group is based on 188 monokaryotic progeny and harbours the phenotypes sporelessness, disturbed orientation of fruiting bodies (geotropism) and the A mating-type.

<https://doi.org/10.1371/journal.pone.0241749.g001>

File) showed that *poMSH4* in the sporulating strain was flanked on the left by a gene encoding a YL1 type nuclear protein and on the right by a sequence representing an open reading frame (ORF) encoding a protein of 660 amino acids containing a CxC5/CxC6 like cysteine cluster. Further downstream in the same region on Sp⁺hap2 scaffold 3, a Long Terminal Repeat (LTR)-retrotransposon (LTR-RT) of the Copia type was found together with additional solo-LTRs of the same Copia type RT. The two overlapping ORFs that were present between the LTRs of the Copia type RT contained all known signatures of a Copia type RT (S2A Fig). The ORF encoding a protein of 660 amino acids containing the CxC5/CxC6 like cysteine cluster that was found at the right flank of *poMSH4* in Sp⁺hap2, was missing at the right flank of the interrupted *poMSH4* in Sp⁻hap2. However, the 6,792 bp “insert” in *poMSH4* of Sp⁻hap2 contained an ORF encoding 739 amino acids, that was very similar to the ORF encoding 660 amino acids at the right flank of *poMSH4* in Sp⁺hap2 (Fig 3B). The “insert” further contained three small, slightly overlapping direct repeats of 46 bp and a cluster of microsatellites with a BC₅NWY signature (Fig 3C). An exact but reversed copy of the 6,792 bp “insert” was also

Table 1. All identified predicted genes located within the 78.9 kb region of the mapped sporeless phenotype.

Nr.	Region in PC15 v2.0 (JGI)	KOG Class	Interpro / KOG description
1	scaffold_03:1007867–1009396	Posttranslational modification, protein turnover, chaperones	
2	scaffold_03:1009681–1010011		
3	scaffold_03:1010157–1011149	Intracellular trafficking, secretion, and vesicular transport	
4	scaffold_03:1012134–1013346	Posttranslational modification, protein turnover, chaperones	Glutathione S-transferase
5	scaffold_03:1013853–1015734	General function prediction only	Protein kinase, core
6	scaffold_03:1016022–1018164	Carbohydrate transport and metabolism	6-phosphogluconate dehydrogenase,
7	scaffold_03:1019029–1020872	Energy production and conversion	FAD linked oxidase,
8	scaffold_03:1022291–1022998	Transcription	Zinc finger, TFIIIS-type
9	scaffold_03:1023761–1024511		
10	scaffold_03:1024915–1027652	Amino acid transport and metabolism	Peptidase M1, membrane alanine aminopeptidase, N-terminal
11	scaffold_03:1027758–1028630	Cytoskeleton	WASP-interacting protein VRP1/WIP, contains WH2 domain
12	scaffold_03:1028626–1029171	Signal transduction mechanisms	Arf GTPase activating protein
13	scaffold_03:1029326–1030398		
14	scaffold_03:1030490–1031232		
15	scaffold_03:1031338–1033801	General function prediction only	DNA-binding protein YL1 and related proteins
16	scaffold_03:1033887–1037750	Replication, recombination and repair	
17	scaffold_03:1038532–1040786	Intracellular trafficking, secretion, and vesicular transport	
18	scaffold_03:1047069–1049837	Posttranslational modification, protein turnover, chaperones	
19	scaffold_03:1060550–1066783	Signal transduction mechanisms	
20	scaffold_03:1066713–1068943	Transcription Regulation	Copper fist DNA binding
21	scaffold_03:1069152–1073123	RNA processing and modification	Ketose-bisphosphate aldolase, class-II
22	scaffold_03:1073942–1076056	Lipid transport and metabolism	Phosphatidylserine decarboxylase-related
23	scaffold_03:1076113–1077336	Posttranslational modification, protein turnover, chaperones	Ubiquitin-conjugating enzyme, E2
24	scaffold_03:1077625–1078856	Coenzyme transport and metabolism	Tetrapyrrole biosynthesis, hydroxymethylbilane synthase
25	scaffold_03:1079274–1079983	Posttranslational modification, protein turnover, chaperones	
26	scaffold_03:1079982–1082435	Posttranslational modification, protein turnover, chaperones	Glycosyl transferase, group 1
27	scaffold_03:1082565–1083606	Translation, ribosomal structure and biogenesis	

Positions are based on the Sp⁺hap2 (http://genome.jgi.doe.gov/PleosPC15_2; [28]) reference sequence. Candidate genes indicated in bold.

<https://doi.org/10.1371/journal.pone.0241749.t001>

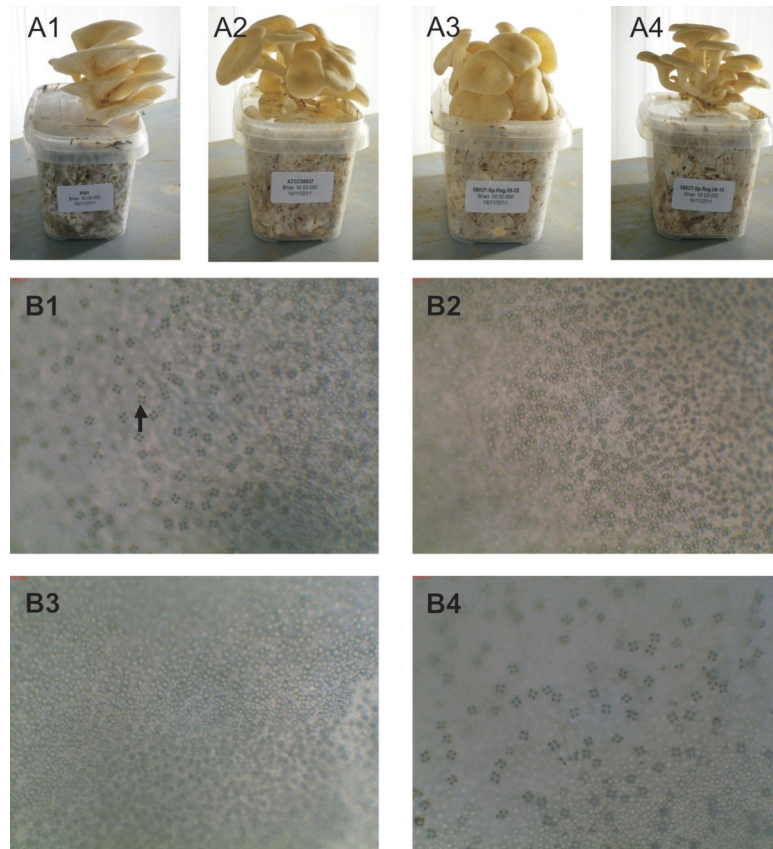


Fig 2. Fruiting bodies and gill tissue of sporulating and non-sporulating strains. Fruiting bodies of the sporulating strain N001 (A1), non-sporulating host ATCC58937 (A2), a transformant containing construct Sp. Reg. 09 showing no restored sporulation (A3) and a transformant containing construct Sp. Reg. 08 harbouring the wild type *poMSH4* gene showing restored sporulation (A4). Microscopic pictures of the gill tissue (20x magnification) of the sporulating strain N001 (B1), non-sporulating host ATCC58937 (B2), a transformant containing construct Sp. Reg. 09 (B3) showing no restored sporulation and a transformant containing construct Sp. Reg. 08 showing restored sporulation (B4). The arrow indicates a tetrad; four spores on top of a basidium.

<https://doi.org/10.1371/journal.pone.0241749.g002>

found 23 kb downstream of the interrupted *poMSH4* gene in Sp⁻hap2. Further differences between the Sp⁻hap2 and the Sp⁺hap2 *poMSH4* regions was the presence of multiple copies of the Copia type RT in Sp⁻hap2; 2 reversed intact copies containing all signatures of Copia type RT (S2B Fig) and 3 partial copies surrounding the downstream copy of the “insert” (Fig 3A and 3B). Finally, 2 solo-LTRs of the Copia type RT were found adjacent to the most right, partial Copia type RT. Upstream of *poMSH4* and further downstream of the most right Copia-LTR, the genomes of Sp⁺hap2 and Sp⁻hap2 were identical.

Cx5/Cx6 like cysteine clusters have been reported to be associated with KDZ-type transposons [42]. However, no transposon of the KDZ-type was found within expected distance of the ORFs encoding the Cx5/Cx6 like cysteine cluster. Using the KDZ-type of transposons previously detected in *Coprinopsis cinerea* and *Laccaria bicolor* [42], tBLASTn revealed the presence of 36 KDZ-type transposons, either truncated or seemingly intact, in the annotated genome of Sp⁺hap2 (http://genome.jgi.doe.gov/PleosPC15_2; [28]). Intact KDZ-type transposons were all preceded by a region encoding a Cx2 cysteine cluster, but never by a Cx5/Cx6 cysteine cluster encoding region (S3 Fig). Regions encoding a Cx5/Cx6 cysteine clusters were also found in high copy numbers throughout the genome. In the wild-type genome (Sp⁺hap2) forty four copies were found, and nearly sixty in the genome of the non-sporulating strain (Sp⁻hap2), either

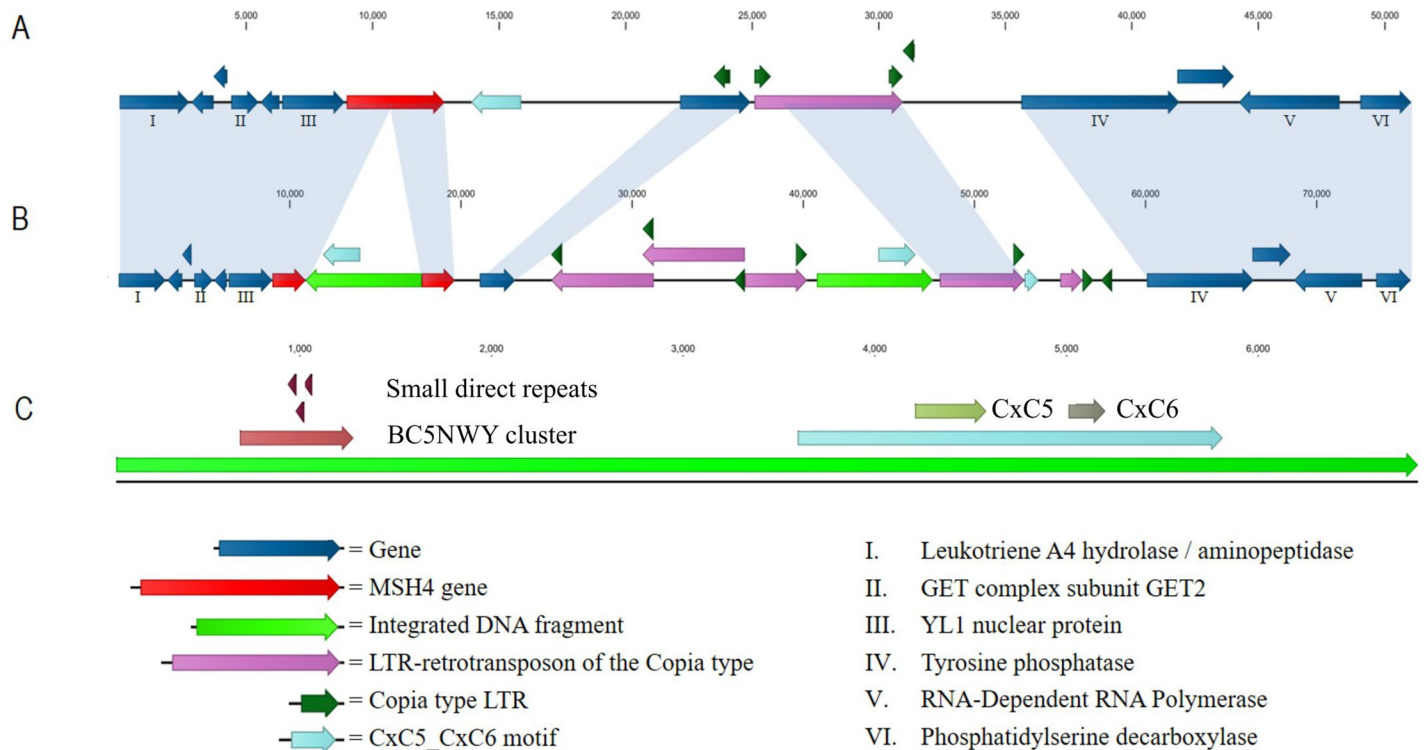


Fig 3. Representation of the annotated sequence of the *poMSH4* region in *Sp*⁺hap2 and *Sp*⁻hap2. Identical genomic sequences between *Sp*⁺hap2 (A) and *Sp*⁻hap2 (B) are indicated with the blue shading. Representation of the 2 identical copies of the integrated DNA fragment of *Sp*⁻hap2 (C).

<https://doi.org/10.1371/journal.pone.0241749.g003>

complete or truncated. Blasting a Copia-type retrotransposon (RT) consensus sequence and the ORF containing the encoded CxC5/CxC6 cysteine cluster to the sequence of the wild-type and the sporeless strain of *P. ostreatus* showed that CxC5/CxC6 cysteine cluster encoding regions are very often associated with the Copia type RT or the LTRs of this Copia-type RT and vice versa. The Copia-type RT and the regions encoding a CxC5/CxC6 cysteine cluster seem not to be distributed randomly over both genomes but are present, often together, in a limited number of spots.

Multiple copies of the DNA fragment integrated in *poMSH4* of *Sp*⁻hap2 are found in the non-sporulating strain as well as the sporulating strain, and are always associated with an intact Copia type retrotransposon

Two additional, full copies of the “insert” were found in the *Sp*⁻hap2 genome on contig 00003652 (S2 File). Both “inserts” are identical and tail-to-tail oriented, 5,897 bp apart (S4 File). Also in *Sp*⁺hap2 (http://genome.jgi.doe.gov/PleosPC15_2; [28]) on scaffold 1 (S5 File) and scaffold 7 (S6 File), a full “insert” is found. When aligned, the major difference between these “inserts” and the DNA fragment integrated in *poMSH4* of *Sp*⁻hap2 is the presence of solo-LTR(s) of the Copia type RT (S4 Fig). But what they all have in common is the presence of at least 1 intact copy of a Copia type RT within a 15 kb distance.

The sporeless *P. ostreatus* mutant ATCC58937 is blocked in the meiotic metaphase I

To examine cytological characteristics of the non-sporulating *P. ostreatus* mutant ATCC58937 (*Sp*⁻dikaryon), the presence of all meiotic stages in the basidia was studied in comparison with

the normal sporulating N001 strain (Sp⁺dikaryon) by light microscopy using HCl-Giemsa stained tissue. In the Sp⁺dikaryon, all developmental processes in the basidia i.e. karyogamy, stages of meiosis I and II, development of sterigmata and the migration of the daughter nuclei to the basidiospores could be identified (Fig 4A). In the Sp⁻dikaryon, meiosis seemed to occur normally up to metaphase I. None of the stages of the meiotic division following the metaphase I could be observed (Fig 4B). The sporeless mutant also seemed incapable of sterigmata formation and basidiospore production.

Construction of a *scMSH4* knock-out in *Schizophyllum commune* results in a strongly reduced sporulation

Protoplasts from germinated spores of a dikaryotic *S. commune* strain $\Delta ku80$ (H4-8/H4-8b background) were transformed with the *scMSH4* deletion construct pDelMSH4 and selected to be nourseothricin resistant and phleomycin sensitive. Screening for phleomycin sensitivity reduces the number of transformants with the pDelMSH4 plasmid integrated outside the target region. PCR analysis showed that 2 out of 8 transformants contained the deleted *scMSH4* ($\Delta MSH4$). Since the transformants were both dikaryotic as a result of unintended protoplast fusion or plasmogamy, they were induced to fructify and monokaryotic progeny was selected on nourseothricin. Monokaryons containing the deleted *scMSH4* and compatible mating-types were selected and crossed to obtain dikaryons homozygous for the interruption. These dikaryons were grown to produce fruiting bodies and their sporulation pattern was studied. In the $\Delta MSH4$ strain, sporulation was strongly reduced (< 2.6 spores/mg wet tissue) when compared to wild-type dikaryons (1808 spores/mg wet tissue).

To confirm that reduction of sporulation is not related to the *ku80* deleted gene, a monokaryon of one of the $\Delta MSH4$ lines was crossed to the isogenic strains H4-8, b, c and d. The crosses that resulted in a dikaryon were selected by looking for clamp connections and were allowed to fructify. Single spore cultures (SSC's) were screened for hygromycin sensitivity (wild type *ku80*) and nourseothricin resistance ($\Delta MSH4$) and were crossed among each other. This resulted in dikaryotic lines with the wild type *ku80* gene in combination with a deleted *scMSH4*. The same was done with hygromycin and nourseothricin sensitive colonies resulting in dikaryotic lines with a wild-type *ku80* in combination with a wild-type *scMSH4*. Five dikaryons were chosen from each group and were further investigated. All the dikaryons homozygous for $\Delta MSH4$ were found to hardly produce any spores when compared to the dikaryons homozygous for wild type *scMSH4* which showed normal sporulation. Except for the strongly reduced sporulation, no phenotypic differences were observed between the dikaryons homozygous for $\Delta MSH4$ and the dikaryons homozygous for wild type *scMSH4*.

Discussion

Transformation of candidate genes to the non-sporulating *P. ostreatus* mutant ATCC58937 (Sp⁻dikaryon) identified the *poMSH4* as the gene responsible for the sporeless phenotype. Comparison of the *poMSH4* sequences of the non-sporulating and the sporulating strain revealed that the *poMSH4* is interrupted by a nearly 7 kb DNA fragment in the non-sporulating mutant. In total 4 copies of this DNA fragment were found in the non-sporulating mutant of which one copy in reversed orientation is located at a 23 kb distance of the copy inserted in *poMSH4*. The other 2 copies are located at a different scaffold, are also tail-to-tail orientated, and are 6 kb apart. Only 2 copies were found in the sporulating strain Sp⁺hap2, each on a different scaffold. All copies of the "insert" DNA fragment contain a region encoding a CxC5/CxC6 cysteine cluster, previously shown to be associated with KDZ-type transposons [42]. However, as all intact KDZ-type transposons were preceded by a region encoding a CxC2



Fig 4. Microscopic pictures of different stages of meiosis in basidia of the sporulating and non-sporulating strains. Sp⁺ dikaryon (A). Binucleated basidium (a), Nuclear fusion (b), Metaphase I—Anaphase I (c), Metaphase I—Anaphase I (d), Telophase I (e), Meta-anaphase II (f, g), Nuclei migrating to spores (h), Binucleate spores after meiotic division (i), and Sp⁻ dikaryon (B). Binucleated basidium (a), Nuclear fusion (b), Different examples of metaphase I (c1-c4). Beyond this stage no examples have been found indicating that meiosis is halted at this stage (Giemsa staining; 100x magnification).

<https://doi.org/10.1371/journal.pone.0241749.g004>

cysteine cluster, but not by a CxC5/CxC6 cysteine cluster encoding region (S3 Fig), this suggests that in *P. ostreatus* the KDZ-type transposon is not associated with CxC5/CxC6 clusters but possibly with CxC2 clusters. The apparent co-localization of the Copia-type RT and the CxC5/CxC6 cysteine cluster encoding region might indicate a cooperation in transposition between these two sequences. Cysteine cluster rich proteins can be involved in recognition of and binding to specific DNA sequences [43] and might explain the presence in specific regions. Alternatively, transposons might multiply within the region of the first copy. The *poMSH4* containing region of the mutated Sp⁻hap2 has clearly been rearranged compared to the same region in the Sp⁺hap2. It is known that transposable elements can mediate genomic rearrangement in many ways [44]. How the rearrangement in the non-sporulating strain was generated is unclear, but seemingly association of Copia RT type transposons and CxC5/CxC6 cysteine cluster encoding regions, and the presence of such a region encoding a CxC5/CxC6 cysteine cluster in the “insert” that disrupts *poMSH4* do indicate that the Copia type RT might have been involved in the disruption.

Microscopic examination (Fig 4) indicates that meiosis is interrupted late in prophase I or metaphase I, which leads to abolishment of all downstream meiotic events and eventually the absence of spores. This also means that somehow, the outcome of meiosis is controlling the process of spore development. In meiosis, the generation of double strand breaks (DSB) leads to recombination between homologous chromosomes that are resolved into non-crossovers (NCOs) or crossovers (COs). In most organisms the majority of DSB are resolved into NCOs [45]. For COs, two distinct pathways have been found in plants, yeast and animals; Class I and Class II. Class I type COs constitute the majority in most organisms and are characterized by the involvement of the so-called ZMM group of proteins that play a role in recombination and formation of the synaptonemal complex (SC) during meiotic prophase I in budding yeast [46], plants [47] and humans [48]. The MSH4-MSH5 heterodimer is part of this complex, that plays a role in stabilizing single-end strand invasion intermediates that are formed during the early stage of recombination, and that binds to Holliday junctions to facilitate crossover formation [49, 50]. The class II type of COs can also resolve Holliday junctions, but is mediated by Mus81-Eme1 proteins and seems to be independent of the ZMM proteins [51]. MSH4 mutants in budding yeast show a delayed SC formation and full synapsis is achieved only in half of all nuclei, leading to a reduction in spore viability of ca. 50% [52]. Mutation of MSH4 generates a similar phenomenon in *Arabidopsis* [47], where the null mutant shows numerous univalents in meiosis, indicating a strong reduction of chromosome pairing due to a strong reduction in chiasmata. The reduced but not complete absence of progeny following mutations in the ZMM proteins (including MSH4) in these organisms has been explained by the still functioning class II crossover pathway [47]. Mutation of MSH4 in mammals leads to complete sterility [46]. Recently, it has been shown in mice that there is a requirement for an intact MSH4-MSH5 heterodimer in crossing over, and also that MSH4-MSH5 is critical for all crossovers, regardless of their starting route from DSB precursors [53]. The role of MSH4 (and likely MSH5) is thus not exactly the same in all eukaryotes. Here we have observed a mutation in the *MSH4* homolog of *P. ostreatus* that causes a null mutation leading to the complete absence of spores. In *S. commune* (in this article) and in *P. pulmonarius* [26], the *MSH4*

mutation leads to a very strong reduction of spores (both <0.1% of the wild type) and indicates a similar role of the encoded proteins in these organisms, which is strengthened by the presence of similar structural domains in the encoded proteins (S5 Fig). Furthermore it may suggest that in basidiomycetes *MSH4* is needed for all type of crossovers or that basidiomycetes do not have a functional (or very inefficient) class II type of CO. The very small number of spores observed in *P. pulmonarius* and *S. commune* might also indicate the existence of additional classes of proteins that can resolve Holliday junctions, but obviously with a very low activity/efficiency.

Most Oyster mushroom varieties show a decrease in yield during prolonged use. The sporeless strain, however, has been continuously cultivated by many growers since its introduction on the market in 2006 and it maintained a high yield. Although speculative, the absence of spores might help explain the stability of the variety. Spores are a known vector for viral diseases in macrofungi [54] including *P. ostreatus* [3]. Different types of viruses have been found in Oyster mushroom crops [3, 55–57] and it is possible that reinfection of crops occur frequently or that even different viral types are accumulated through lingering spores when using different varieties over time. The generation of a sporeless Oyster mushroom variety by introduction of the natural mutation has led to a commercially successful Oyster mushroom variety that is now used by many growers in Europe. The disturbed orientation of Oyster mushrooms within bunches of the sporeless variety could be considered as less beautiful, although most harvested mushrooms are packed as individual mushrooms rendering disturbed orientation irrelevant. Mapping the phenotypes sporelessness and disturbed orientation revealed that both phenotypes are tightly linked. Moreover, introducing a wild type *poMSH4* gene in the sporeless strain restored sporulation as well as the orientation of the fruiting bodies. This indicates that the block in meiosis and absence of spores relate to the disturbed orientation. Gravitropic bending in mushrooms either by stipe or fruiting body is a prerequisite for optimal spore dispersal [58]. How the absence of spores relates to the disturbed orientation remains unknown. In *S. commune* the relationship between *scMSH4* and fruiting body morphology could not be studied since strain H4-8, used as host for transformation, is already disturbed in its response to gravity. Okuda et al. reported no effect on fruiting body morphology after a knock-out of a *MSH4* homolog in *P. pulmonarius* [26]. However, no bunches of fruiting bodies were shown in their publication. Obatake et al. generated a sporeless *P. eryngii* mutant by UV irradiation [16]. It appeared to be a dominant mutation that also blocked meiosis in metaphase I causing the absence of sterigmata and spores. Interestingly, they observed a deviation from the wild type mushrooms, i.e. mushrooms seemed to have lost a bit of their negative gravitropy and did not grow completely perpendicular in the substrate (“leaning mushrooms” as they call it). This might suggest that, whatever mutation is used to block sporulation, the interruption of meiosis and or the absence of spores can affect the orientation of mushrooms. As for *P. ostreatus*, also for *P. eryngii* the effect is not seen after harvest and packing of individual mushrooms. *MSH4* homologs might thus be a good candidate to generate also sporeless varieties in other edible basidiomycetes. Since the obvious method to generate knockouts, i.e. CRISPR Cas9, is not an breeding method accepted by most consumers, mutants should be obtained in classical ways. Strains of these species containing a mutated *MSH4* homolog may be obtained by screening a natural strain collection for *MSH4* homolog mutants. In addition, the mutant may also be obtained by classical mutagenesis approaches followed by high-throughput screening of this mutant library, as suggested before [26]. This marker can then be used for breeding, following a similar strategy as described for *P. ostreatus* [18, 19, 21] which resulted in a marketable sporeless strain.

Supporting information

S1 Fig. Genetic linkage map of Sp⁺Hap2 x Sp⁻Hap2. The linkage map is based on 188 mono-karyotic progeny of the cross using 387 genetic markers and the phenotypes A mating-type, B mating-type, sporelessness and disturbed orientation of fruiting bodies (geotropism). (TIF)

S2 Fig. Identified signatures in the LTR to LTR retrotransposon of the Copia-type. The retrotransposons located in the *poMSH4* region of Sp⁺hap2 (A) and Sp⁻hap2 (B). (TIF)

S3 Fig. Annotation of the ORFs of the KDZ-type transposons found in the annotated sequence of the Sp⁺hap2. http://genome.jgi.doe.gov/PleosPC15_2. (TIF)

S4 Fig. Alignment of all copies of the “insert” found in Sp⁻hap2 and Sp⁺hap2. Insert_1_1 and insert_1_2 are identical copies, located in the *poMSH4* region of Sp⁻hap2 (contig 00000008) of which insert_1_1 is integrated into *poMSH4*, disrupting the gene. Insert_2_1 and insert_2_2 are identical copies, located on contig 00003652 of Sp⁻hap2. Major difference between the “inserts” located in the *poMSH4* region of Sp⁻hap2 and all the other copies of the “insert” is the absence of solo-LTRs of the Copia type RT (dark green). Next to that, there are some small differences in the number and composition of the small repeat units with the BC5NWY signature (Dark red). The light blue region represents the CxC5/CxC6 cysteine cluster encoding region with the CxC5 domain (light green) and the CxC6 domain (grey). (TIF)

S5 Fig. CLUSTAL multiple sequence alignment between the *P. ostreatus poMSH4*, *P. pulmonarius stpp1* (accession no. AB761293) and *S. commune scMSH4*. Conserved domains indicated as described by Okuda *et al.* [26]. The olive green boxes represent the ATP binding site and the stale blue represents the ABC transporter signature motif. Hash tags, upward-pointing arrows, downward-pointing arrows, plus signs and asterisks indicate the Walker A, Walker B, D-loop, Q-loop and H-loop respectively. (PDF)

S1 Table. Primer combinations used in vector construction for transformation to *P. ostreatus* strain ATCC58937. Primers were designed to amplify genes including a 1 kb promoter and 500 bp terminator region using *Pleurotus ostreatus* Sp⁺hap2 as template. (DOCX)

S2 Table. Primer combinations for screening *P. ostreatus* transformants for the presence of the candidate gene(s). (DOCX)

S3 Table. Primer combinations for construction of the deletion vector (pDelMSH4) and for screening *S. commune scMSH4* transformants. (DOCX)

S1 File. MSH4_region_PleosPC15_2. Sequence of the *poMSH4* region of the WT *P. ostreatus* strain (Sp⁺hap2). (GBK)

S2 File. Draft assembly of pleosEP57. (FASTA)

S3 File. MSH4_region_EP57. Sequence of the *poMSH4* region of the *P. ostreatus* mutant strain (Sp⁻hap2).
(GBK)

S4 File. Insert_2_region_EP57. Sequence of the region of the *P. ostreatus* mutant strain (Sp⁻hap2) from contig 00003652 containing the additional copies of the “insert”.
(GBK)

S5 File. PC15_insert_Sc01. Sequence of the “insert” homolog region on scaffold 1 of the WT *P. ostreatus* strain (Sp⁺hap2).
(GBK)

S6 File. PC15_insert_Sc07. Sequence of the “insert” homolog region on scaffold 7 of the WT *P. ostreatus* strain (Sp⁺hap2).
(GBK)

Acknowledgments

The authors thank Patrick Hendrickx for his assistance in generating a genetic linkage map and Ed Hendriks and José Kuenen for their technical assistance in *P. ostreatus* cultivation. Additionally, the authors thank Yoichi Honda and Thomas Mikosch for their expertise and help in setting up a *P. ostreatus* transformation protocol.

Author Contributions

Conceptualization: Anton S. M. Sonnenberg.

Formal analysis: Brian Lavrijssen.

Investigation: Brian Lavrijssen, Luis G. Lugones, Narges Sedaghat Telgerd.

Methodology: Brian Lavrijssen.

Supervision: Arend F. van Peer.

Writing – original draft: Brian Lavrijssen, Luis G. Lugones, Karin Scholtmeijer, Anton S. M. Sonnenberg, Arend F. van Peer.

Writing – review & editing: Johan P. Baars, Karin Scholtmeijer, Anton S. M. Sonnenberg, Arend F. van Peer.

References

1. Cox A, Folgering HT, van Griensven LJ. Extrinsic allergic alveolitis caused by spores of the oyster mushroom *Pleurotus ostreatus*. *Eur Respir J*. 1988; 1(5):466–8. Epub 1988/05/01. PMID: [3169217](https://pubmed.ncbi.nlm.nih.gov/3169217/).
2. Grogan HM, Adie BA, Gaze RH, Challen MP, Mills PR. Double-stranded RNA elements associated with the MVX disease of *Agaricus bisporus*. *Mycol Res*. 2003; 107(Pt 2):147–54. Epub 2003/05/16. <https://doi.org/10.1017/s0953756203007202> PMID: [12747325](https://pubmed.ncbi.nlm.nih.gov/12747325/).
3. Kim YJ, Kim JY, Kim JH, Yoon SM, Yoo YB, Yie SW. The identification of a novel *Pleurotus ostreatus* dsRNA virus and determination of the distribution of viruses in mushroom spores. *J Microbiol*. 2008; 46(1):95–9. Epub 2008/03/14. <https://doi.org/10.1007/s12275-007-0171-y> PMID: [18337700](https://pubmed.ncbi.nlm.nih.gov/18337700/).
4. Royse DJ, Baars J, Tan Q. Current Overview of Mushroom Production in the World. In: Diego CZ, Pardo-Giménez A, editors. *Edible and Medicinal Mushrooms 2017*. p. 5–13.
5. Sonnenberg ASM, van Loon PCC, van Griensven LJLD. The number of spores spread by *Pleurotus* spp. in the air / Het aantal sporen dat *Pleurotus* spp. in de lucht verspreid. *De Champignoncultuur*. 1996; 40(7):269–72.

6. Verrinder Gibbins AM, Lu BC. An ameiotic mutant of *Coprinus cinereus* halted prior to pre-meiotic S-phase. *Curr Genet.* 1982; 5(2):119–26. Epub 1982/07/01. <https://doi.org/10.1007/BF00365702> PMID: 24186227.
7. Bromberg SK, Schwalb MN. Isolation and Characterization of Temperature Sensitive Sporulationless Mutants of the Basidiomycete *Schizophyllum Commune*. *Canadian Journal of Genetics and Cytology.* 1977; 19(3):477–81. <https://doi.org/10.1139/g77-051>
8. Hasebe K, Murakami S, Tsuneda A. Cytology and Genetics of a Sporeless Mutant of *Lentinus-Edodes*. *Mycologia.* 1991; 83(3):354–9. <https://doi.org/10.2307/3759995> WOS:A1991FU07600012.
9. Chen WM, Zhang XL, Chai HM, Chen LJ, Liu WL, Zhao YC. Comparative Analysis of Sporulating and Spore-Deficient Strains of *Agrocybe salicicola* Based on the Transcriptome Sequences. *Curr Microbiol.* 2015; 71(2):204–13. Epub 2015/04/24. <https://doi.org/10.1007/s00284-015-0819-5> PMID: 25903265
10. Eger G, Eden G, Wissig E. *Pleurotus Ostreatus*—breeding potential of a new cultivated mushroom. *Theor Appl Genet.* 1976; 47(4):155–63. Epub 1976/07/01. <https://doi.org/10.1007/BF00278373> PMID: 24414617.
11. Ohira I. Sporulation-Deficient Mutant in *Pleurotus-Pulmonarius* Fr. *T Mycol Soc Jpn.* 1979; 20(2):107–14. WOS:A1979HX08100001.
12. Kanda T, Goto A, Sawa K, Arakawa H, Yasuda Y, Takemaru T. Isolation and Characterization of Recessive Sporeless Mutants in the Basidiomycete *Coprinus-Cinereus*. *Mol Gen Genet.* 1989; 216(2–3):526–9. <https://doi.org/10.1007/Bf00334400> WOS:A1989U365500047.
13. Murakami S. Genetics and breeding of spore deficient strains in *Agrocybe cylindracea* and *Lentinus edodes*. In: Chang ST, Buswell JA, Chiu SW, editors. *Mushroom biology and mushroom products: The Chinese University Press, Hong Kong, China; 1993. p. 63–9.*
14. Imbernon M, Labarere J. Selection of sporeless or poorly-spored induced mutants from *Pleurotus ostreatus* and *Pleurotus pulmonarius* and selective breeding. *Mushroom Science.* 1989; XII:109–23.
15. Joh JH, Kim BG, Kong WS, Yoo YB, Chu KS, Kim NK, et al. Isolation and Characterization of Dikaryotic Mutants from *Pleurotus ostreatus* by UV Irradiation. *Mycobiology.* 2004; 32(2):88–94. <https://doi.org/10.4489/myco.2004.32.2.088>
16. Obatake Y, Murakami S, Matsumoto T, Fukumasa-Nakai Y. Isolation and characterization of a sporeless mutant in *Pleurotus eryngii*. *Mycoscience.* 2003; 44(1):33–40. <https://doi.org/10.1007/s10267-002-0074-z>
17. Pandey M, Ravishankar S. Development of sporeless and low-spored mutants of edible mushroom for alleviating respiratory allergies. *Current Science.* 2010; 99(10):1449–53. WOS:000285081400038.
18. Baars JJP, Hendrickx PM, Sonnenberg ASM. Prototype of a Sporeless Oyster Mushroom. *Mushroom Science.* 2004; XVI:139–47.
19. Baars JJP, Heslen H. Experience with sporeless strains of oyster mushroom (*Pleurotus ostreatus*) in commercial production. *Mushroom Science.* 2008; XVII:774–87.
20. Obatake Y, Murakami S, Matsumoto T, Fukumasa Y. Development of a sporeless strain of *Pleurotus eryngii*. *Nihon Kingakkai Nishinohon Shibukaiho [In Japanese].* 2006; 15:18–27.
21. Baars JJP, Sonnenberg ASM, Mikosch TSP, van Griensven LJLD. Development of a sporeless strain of oyster mushroom *Pleurotus ostreatus*. *Mushroom Science.* 2000; XV:317–23.
22. Mikosch TSP, Sonnenberg ASM, Van Griensven LJLD. Isolation, Characterization, and Expression Patterns of a DMC1 Homolog from the Basidiomycete *Pleurotus ostreatus*. *Fungal Genet Biol.* 2001; 33(1):59–66. Epub 2001/06/16. <https://doi.org/10.1006/fgbi.2001.1265> PMID: 11407886.
23. Cummings WJ, Celerin M, Crodian J, Brunick LK, Zolan ME. Insertional mutagenesis in *Coprinus cinereus*: use of a dominant selectable marker to generate tagged, sporulation-defective mutants. *Curr Genet.* 1999; 36(6):371–82. Epub 2000/02/02. <https://doi.org/10.1007/s002940050512> PMID: 10654091.
24. Mikosch TSP, Sonnenberg ASM, Van Griensven LJLD. Isolation, characterisation and expression patterns of a RAD51 ortholog from *Pleurotus ostreatus*. *Mycological Research.* 2002; 106(6):682–7. <https://doi.org/10.1017/s0953756202005877>
25. Sugawara H, Iwabata K, Koshiyama A, Yanai T, Daikuhara Y, Namekawa SH, et al. *Coprinus cinereus* Mer3 is required for synaptonemal complex formation during meiosis. *Chromosoma.* 2009; 118(1):127–39. Epub 2008/10/09. <https://doi.org/10.1007/s00412-008-0185-1> PMID: 18841377.
26. Okuda Y, Murakami S, Honda Y, Matsumoto T. An *MSH4* homolog, *stpp1*, from *Pleurotus pulmonarius* is a "silver bullet" for resolving problems caused by spores in cultivated mushrooms. *Appl Environ Microbiol.* 2013; 79(15):4520–7. Epub 2013/05/15. <https://doi.org/10.1128/AEM.00561-13> PMID: 23666334; PubMed Central PMCID: PMC3719512.
27. Larraya LM, Perez G, Penas MM, Baars JJ, Mikosch TS, Pisabarro AG, et al. Molecular karyotype of the white rot fungus *Pleurotus ostreatus*. *Appl Environ Microbiol.* 1999; 65(8):3413–7. Epub 1999/07/

31. <https://doi.org/10.1128/AEM.65.8.3413-3417.1999> PMID: 10427028; PubMed Central PMCID: PMC91513.
28. Alfaro M, Castanera R, Lavin JL, Grigoriev IV, Oguiza JA, Ramirez L, et al. Comparative and transcriptional analysis of the predicted secretome in the lignocellulose-degrading basidiomycete fungus *Pleurotus ostreatus*. *Environ Microbiol*. 2016; 18(12):4710–26. Epub 2016/04/28. <https://doi.org/10.1111/1462-2920.13360> PMID: 27117896.
29. de Jong JF, Ohm RA, de Bekker C, Wosten HA, Lugones LG. Inactivation of ku80 in the mushroom-forming fungus *Schizophyllum commune* increases the relative incidence of homologous recombination. *FEMS Microbiol Lett*. 2010; 310(1):91–5. Epub 2010/07/29. <https://doi.org/10.1111/j.1574-6968.2010.02052.x> PMID: 20662932.
30. Dons JJM, De Vries OMH, Wessels JGH. Characterization of the genome of the basidiomycete *Schizophyllum commune*. *Biochimica et Biophysica Acta (BBA)—Nucleic Acids and Protein Synthesis*. 1979; 563(1):100–12. [https://doi.org/10.1016/0005-2787\(79\)90011-x](https://doi.org/10.1016/0005-2787(79)90011-x) PMID: 574021
31. Stam P. Construction of integrated genetic linkage maps by means of a new computer package: Join Map. *The Plant Journal*. 1993; 3(5):739–44. <https://doi.org/10.1111/j.1365-313X.1993.00739.x>
32. van Peer AF, Park SY, Shin PG, Jang KY, Yoo YB, Park YJ, et al. Comparative genomics of the mating-type loci of the mushroom *Flammulina velutipes* reveals widespread synteny and recent inversions. *PLOS ONE*. 2011; 6(7):e22249. Epub 2011/07/30. <https://doi.org/10.1371/journal.pone.0022249> PMID: 21799803; PubMed Central PMCID: PMC3140503.
33. Koren S, Walenz BP, Berlin K, Miller JR, Bergman NH, Phillippy AM. Canu: scalable and accurate long-read assembly via adaptive k-mer weighting and repeat separation. *Genome Res*. 2017; 27(5):722–36. Epub 2017/03/17. <https://doi.org/10.1101/gr.215087.116> PMID: 28298431; PubMed Central PMCID: PMC5411767.
34. Sonnenberg AS, Wessels JG, van Griensven LJ. An efficient protoplasting/regeneration system for *Agaricus bisporus* and *Agaricus bitorquis*. *Current Microbiology*. 1988; 17(5):285–91. <https://doi.org/10.1007/bf01571330>
35. Binnering DM, Skrzynia C, Pukkila PJ, Casselton LA. DNA-mediated transformation of the basidiomycete *Coprinus cinereus*. *The EMBO Journal*. 1987; 6(4):835–40. <https://doi.org/10.1002/j.1460-2075.1987.tb04828.x> PMID: 3595558
36. Sonnenberg ASM, Wessels JGH. Heterokaryon formation in the basidiomycete *Schizophyllum commune* by electrofusion of protoplasts. *Theor Appl Genet*. 1987; 74(5):654–8. Epub 1987/09/01. <https://doi.org/10.1007/BF00288866> PMID: 24240223.
37. Irie T, Honda Y, Watanabe T, Kuwahara M. Efficient transformation of filamentous fungus *Pleurotus ostreatus* using single-strand carrier DNA. *Appl Microbiol Biotechnol*. 2001; 55(5):563–5. Epub 2001/06/21. <https://doi.org/10.1007/s002530000535> PMID: 11414321.
38. Honda Y, Matsuyama T, Irie T, Watanabe T, Kuwahara M. Carboxin resistance transformation of the homobasidiomycete fungus *Pleurotus ostreatus*. *Curr Genet*. 2000; 37(3):209–12. Epub 2000/05/04. <https://doi.org/10.1007/s002940050521> PMID: 10794179.
39. Ohm RA, de Jong JF, Berends E, Wang F, Wosten HA, Lugones LG. An efficient gene deletion procedure for the mushroom-forming basidiomycete *Schizophyllum commune*. *World J Microbiol Biotechnol*. 2010; 26(10):1919–23. Epub 2010/10/12. <https://doi.org/10.1007/s11274-010-0356-0> PMID: 20930926; PubMed Central PMCID: PMC2940052.
40. Sokolovsky V, Kaldenhoff R, Ricci M, Russo VEA. Fast and reliable mini-prep RNA extraction from *Neurospora crassa*. *Fungal Genetics Reports*. 1990; 37(1):41–3. <https://doi.org/10.4148/1941-4765.1492>
41. Sivolapova AB, Shnyreva AV, Sonnenberg A, Baars I. DNA marking of some quantitative trait loci in the cultivated edible mushroom *Pleurotus ostreatus* (Fr.) Kumm. *Russian Journal of Genetics*. 2012; 48(4):383–9. <https://doi.org/10.1134/S1022795412040114> WOS:000303468000004.
42. Iyer LM, Zhang D, de Souza RF, Pukkila PJ, Rao A, Aravind L. Lineage-specific expansions of TET/JBP genes and a new class of DNA transposons shape fungal genomic and epigenetic landscapes. *Proc Natl Acad Sci U S A*. 2014; 111(5):1676–83. Epub 2014/01/09. <https://doi.org/10.1073/pnas.1321818111> PMID: 24398522; PubMed Central PMCID: PMC3918813.
43. MacPherson S, Laroche M, Turcotte B. A fungal family of transcriptional regulators: the zinc cluster proteins. *Microbiol Mol Biol Rev*. 2006; 70(3):583–604. Epub 2006/09/09. <https://doi.org/10.1128/MMBR.00015-06> PMID: 16959962; PubMed Central PMCID: PMC1594591.
44. Gray YH. It takes two transposons to tango: transposable-element-mediated chromosomal rearrangements. *Trends Genet*. 2000; 16(10):461–8. Epub 2000/10/26. [https://doi.org/10.1016/s0168-9525\(00\)02104-1](https://doi.org/10.1016/s0168-9525(00)02104-1) PMID: 11050333.
45. Bolcun-Filas E, Handel MA. Meiosis: the chromosomal foundation of reproduction. *Biol Reprod*. 2018; 99(1):112–26. Epub 2018/02/01. <https://doi.org/10.1093/biolre/iy021> PMID: 29385397.

46. Kneitz B, Cohen PE, Avdievich E, Zhu L, Kane MF, Hou H Jr., et al. MutS homolog 4 localization to meiotic chromosomes is required for chromosome pairing during meiosis in male and female mice. *Genes Dev.* 2000; 14(9):1085–97. Epub 2000/05/16. PMID: [10809667](https://pubmed.ncbi.nlm.nih.gov/10809667/); PubMed Central PMCID: PMC316572.
47. Higgins JD, Armstrong SJ, Franklin FC, Jones GH. The Arabidopsis MutS homolog AtMSH4 functions at an early step in recombination: evidence for two classes of recombination in Arabidopsis. *Genes Dev.* 2004; 18(20):2557–70. Epub 2004/10/19. <https://doi.org/10.1101/gad.317504> PMID: [15489296](https://pubmed.ncbi.nlm.nih.gov/15489296/); PubMed Central PMCID: PMC529542.
48. Bocker T. hMSH5: A human MutS homologue that forms a novel heterodimer with hMSH4 and is expressed during spermatogenesis. *Cancer Research.* 1999; 59(4):816–22. PMID: [10029069](https://pubmed.ncbi.nlm.nih.gov/10029069/)
49. Snowden T, Acharya S, Butz C, Berardini M, Fishel R. hMSH4-hMSH5 recognizes Holliday Junctions and forms a meiosis-specific sliding clamp that embraces homologous chromosomes. *Mol Cell.* 2004; 15(3):437–51. Epub 2004/08/12. <https://doi.org/10.1016/j.molcel.2004.06.040> PMID: [15304223](https://pubmed.ncbi.nlm.nih.gov/15304223/).
50. Nishant KT, Chen C, Shinohara M, Shinohara A, Alani E. Genetic analysis of baker's yeast Msh4-Msh5 reveals a threshold crossover level for meiotic viability. *PLoS Genet.* 2010; 6(8):e1001083. Epub 2010/09/25. <https://doi.org/10.1371/journal.pgen.1001083> PMID: [20865162](https://pubmed.ncbi.nlm.nih.gov/20865162/); PubMed Central PMCID: PMC2928781.
51. Mercier R, Mezard C, Jenczewski E, Macaisne N, Grelon M. The molecular biology of meiosis in plants. *Annu Rev Plant Biol.* 2015; 66(1):297–327. Epub 2014/12/11. <https://doi.org/10.1146/annurev-arplant-050213-035923> PMID: [25494464](https://pubmed.ncbi.nlm.nih.gov/25494464/).
52. Novak JE, Ross-Macdonald PB, Roeder GS. The budding yeast Msh4 protein functions in chromosome synapsis and the regulation of crossover distribution. *Genetics.* 2001; 158(3):1013–25. Epub 2001/07/17. PMID: [11454751](https://pubmed.ncbi.nlm.nih.gov/11454751/); PubMed Central PMCID: PMC1461720.
53. Milano CR, Holloway JK, Zhang Y, Jin B, Smith C, Bergman A, et al. Mutation of the ATPase Domain of MutS Homolog-5 (MSH5) Reveals a Requirement for a Functional MutSgamma Complex for All Cross-overs in Mammalian Meiosis. *G3 (Bethesda).* 2019; 9(6):1839–50. Epub 2019/04/05. <https://doi.org/10.1534/g3.119.400074> PMID: [30944090](https://pubmed.ncbi.nlm.nih.gov/30944090/); PubMed Central PMCID: PMC6553527.
54. Sahin E, Akata I. Viruses infecting macrofungi. *Virusdisease.* 2018; 29(1):1–18. Epub 2018/04/03. <https://doi.org/10.1007/s13337-018-0434-8> PMID: [29607353](https://pubmed.ncbi.nlm.nih.gov/29607353/); PubMed Central PMCID: PMC5877858.
55. van der Lende TR, Harmsen MC, Go SJ, Wessels JGH, Wessel JG. Double-stranded RNA mycoviruses in mycelium of *Pleurotus ostreatus*. *FEMS Microbiol Lett.* 1995; 125(1):51–6. Epub 1995/01/01. <https://doi.org/10.1111/j.1574-6968.1995.tb07334.x> PMID: [7867920](https://pubmed.ncbi.nlm.nih.gov/7867920/).
56. Yu HJ, Lim D, Lee HS. Characterization of a novel single-stranded RNA mycovirus in *Pleurotus ostreatus*. *Virology.* 2003; 314(1):9–15. Epub 2003/10/01. [https://doi.org/10.1016/s0042-6822\(03\)00382-9](https://doi.org/10.1016/s0042-6822(03)00382-9) PMID: [14517055](https://pubmed.ncbi.nlm.nih.gov/14517055/).
57. Ro HS, Lee NJ, Lee CW, Lee HS. Isolation of a novel mycovirus OMIV in *Pleurotus ostreatus* and its detection using a triple antibody sandwich-ELISA. *J Virol Methods.* 2006; 138(1–2):24–9. Epub 2006/08/26. <https://doi.org/10.1016/j.jviromet.2006.07.016> PMID: [16930731](https://pubmed.ncbi.nlm.nih.gov/16930731/).
58. Hock B, Häder D-P. Gravidresponses in fungi and slime molds. *Signal Transduction.* 2006; 6(6):443–8. <https://doi.org/10.1002/sita.200600111>